

# Optical Emissions from Burning Jet Fuel

R.M.F. Linford\* and C.F. Dillow†  
*McDonnell Douglas Corporation, St. Louis, Mo.*

and  
T.M. Trumble‡  
*Air Force Aero Propulsion Laboratory, Wright Patterson AFB, Ohio*

A series of experiments is described in which the spectral radiant intensity of burning JP-4 is measured in the spectral region from 200 nm to 15  $\mu\text{m}$ . Spectral data are presented for small diffusion flames burning at various simulated altitudes ranging from sea level to 10.7 km. Pronounced band spectra attributable to the CO and OH radicals characterize the ultraviolet (200–310 nm) emissions which are found to increase in intensity at higher altitudes. A broadband continuum exists throughout the remainder of the spectral region examined (310 nm–15  $\mu\text{m}$ ) and its intensity is seen to decrease at higher altitudes. An extremely intense  $\text{CO}_2$  emission band at 4.4  $\mu\text{m}$  is of primary interest in this region and its possible use for fire detection is discussed.

## Introduction

**O**PTICAL sensors are strong candidates as the basic element of fire detection systems for both military and commercial aircraft. Fuels, lubricants, and hydraulic fluids are all present in copious quantities in modern aircraft and most of these materials are highly flammable. In the event of a fire these fluids burn with a bright open flame, and can be detected readily with an appropriate optical sensor. However, an operational fire detection system must not only detect flames but must also discriminate effectively against background radiation such as sunlight, artificial lighting, gunfire, sparks, or radiation from hot surfaces in the field of view of the detector.

For the designer of a fire detection system to be able to balance the conflicting requirements of detecting a fire while ignoring the background, he must have detailed information on each of the following parameters: the spectral calibration of the sensor, the spectral radiant intensity of the fire, and details of the likely sources of background radiation.

Of these parameters, the radiation emitted by aircraft fires is the most difficult to predict. Flame spectroscopy is a long established branch of science, dating back to the work of men such as Bunsen, Herschel, and Kirchhoff, and esoteric contributions to the subject appear frequently in the pages of technical journals. However, the emphasis of much of the work in this area has been on the analyses of combustion phenomena by identification of chemical species in the flame, with an occasional measurement of the relative intensities of prominent spectral peaks. The designer of a fire detection system is not concerned with the reaction chemistry of flames, but does have a requirement for quantitative spectral radiant intensity data for potential fires. Despite the long history of work in the combustion area, only limited data have been published for JP-4 and other burning aircraft fluids.

The experiments described in this paper were designed to determine the spectral radiant intensity of small diffusion flames of JP-4 aviation jet fuel burning in atmospheres which simulated altitudes ranging from sea level to 10.7 km (35,000 ft). Data were taken at wavelengths from the middle ultraviolet (0.2  $\mu\text{m}$ ) to the far infrared (15  $\mu\text{m}$ ).

## Experimental Details

### Combustion and Fuel Handling Systems

The design of the combustion system is crucial to all flame spectroscopy, but was particularly important in our tests where a small diffusion flame was generated to represent an aircraft fire at simulated altitudes up to 10.7 km (35,000 ft). It was also important that the optical system collected radiation from all portions of the flame, so the optical system field of view became a major constraint on the flame dimensions. Following experiments with a variety of nozzles and fuel flowrates, a flame 175 mm tall was selected, corresponding to a fuel flowrate of approximately 0.25  $\text{cm}^3/\text{min}$  through a 0.075 mm diameter nozzle.

Fuel from a nitrogen-pressurized reservoir was forced through a commercial oil-burner§ nozzle fitted with a 0.075 mm aperture. A nichrome wire heater was wound on the nozzle assembly and potted in ceramic paste. Fuel ignition was achieved with a spark between two wire electrodes set approximately 20 mm apart and 30 mm above the nozzle and connected to a 15 kV neon-sign transformer. A nozzle temperature of approximately 95°C, and an 80-torr differential pressure between the reservoir and the combustion chamber resulted in stable flames which would burn for several hours without interruption.

The nozzle assembly was installed in a high-altitude combustion chamber, as depicted in Fig. 1. For sea-level measurements the extension snout and the top and bottom vacuum flanges were removed, and a portable fume hood was positioned atop the chamber to remove the soot and gases generated by the flame. The purpose of the extension snout was to achieve the required field of view with a 75 mm diameter optical window.

A primary concern during the high-altitude measurements was that an adequate supply of oxygen be continually available for full combustion of the JP-4. Moreover the fresh air supply had to be provided without perturbing the flame, which would result in noise in the electro-optical measuring system. These requirements were satisfied by evacuating the chamber with an 8 liters/sec (15  $\text{ft}^3/\text{min}$ ) mechanical pump through a port in the top plate, while allowing fresh air to enter at the bottom through a throttle valve and then through an automotive air filter, thus minimizing air turbulence. A second automotive air filter was employed in the pumping line to prevent dense black smoke from entering the mechanical pump. The pressure in the chamber was adjusted with the

Received Sept. 15, 1975; revision received Jan. 14, 1977.

Index categories: Fuels and Propellants, Properties of; Fuels and Fuel Systems; Safety.

\*Unit Chief, Member AIAA.

†Test Engineer.

‡Chief-Instrumentation Group.

§Delavan Manufacturing Company, Des Moines, Iowa.

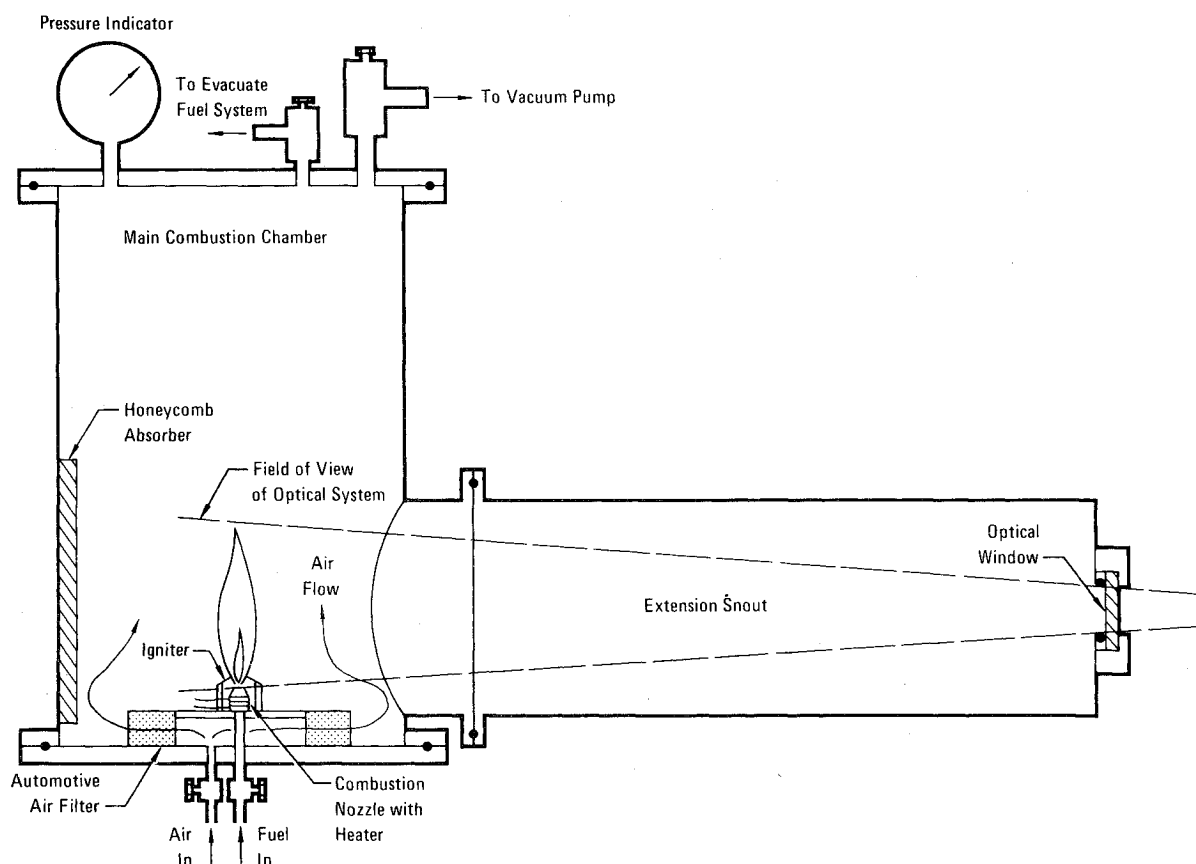


Fig. 1 High-altitude combustion chamber.

throttle valve and measured with a Wallace and Tiernan dial gage.

A calculation of the effective speed of the pumping system indicated that approximately 10 liters/min of air was drawn through the chamber. Using a simplified molecular structure for JP-4,  $C_8H_{18}$ , it was calculated that  $0.2 \text{ cm}^3/\text{min}$  of the fuel would require approximately 2.5 liters/min of fresh air for complete combustion. To confirm that adequate air was drawn through the chamber, the optical output from a JP-4 flame burning at 10.7 km (190 torr) was monitored for a period of time following ignition. No systematic variations in the level of optical energy emitted by the flame were detected for a period of more than an hour, indicating that the flame was not starved of oxygen. This test also confirmed that negligible contamination of the optical window occurred.

#### Optical System

A fire detector will view all emitted radiation and therefore it was important that the optical measurements be made on the entire flame rather than a select portion. The requirement to measure the absolute radiant intensity of the flame also required frequent calibration with a standard source. The system designed to meet these requirements is shown in Fig. 2. The version of the optical system shown here was used for the ultraviolet, visible, and near infrared measurements ( $0.2\text{--}2.6 \mu\text{m}$ ). Radiation from the flame was directed onto the entrance slit of a Jarrell-Ash half-meter grating spectrometer equipped with either a lead sulfide or a photomultiplier detector. The use of the flip mirror allowed direct comparison of the flame with a radiant intensity standard on the other arm of the tee.

Other features of the optical system in Fig. 2 are the 660-Hz chopper to facilitate the use of lock-in amplification of the detector outputs; a high quality synthetic fused silica window<sup>1</sup> on the combustion chamber and a matching com-

pensation window in the calibration system; and a honeycomb absorber behind the flame to eliminate stray reflections.

A secondary spectral radiant intensity standard was provided by the optical system shown in the upper right-hand corner of Fig. 2. A full-size image of the tungsten strip filament of a G.E. 30A/T24 lamp was formed by the  $f/10$  optical system in the plane of the exit aperture. The radiance of this image was calibrated against a spectral radiance standard certified by the National Bureau of Standards. When a portion of this image was selected by a precision aperture a secondary radiant intensity standard was established.

For far-infrared measurements the grating spectrometer was replaced by a Block Engineering Model 195T Infrared Emission Spectrometer. This instrument is basically an interferometer cube with an oscillating mirror and a built-in thermistor detector. The output of the detector is in the form of a complex interferogram and must be analyzed by a fast Fourier transform computer program to determine the spectrum of the incident radiation. For spectral calibration of the spectrometer an Electro Optical Industries 1000 °C blackbody was installed in one arm of the optical system and a 10 mm water-cooled aperture served as the radiant intensity standard. Potassium bromide windows were used in place of silica for the infrared measurements.

Details of the detectors, order filters, and gratings used are listed in Table 1. The division of the spectrum into ten ranges was made to accommodate the many order-of-magnitude variations in the emitted radiation across the entire range, and to accommodate the performance limits of the various optical components.

#### Data Acquisition and Reduction

The outputs of the detectors were recorded in the memory of a Nicolet Corporation Model 1072 Instrument Computer, and then stored on magnetic tape. Before each scan of the

<sup>1</sup>6 mm-thick Suprasil 2 supplied by Amersil, Inc., New Jersey.

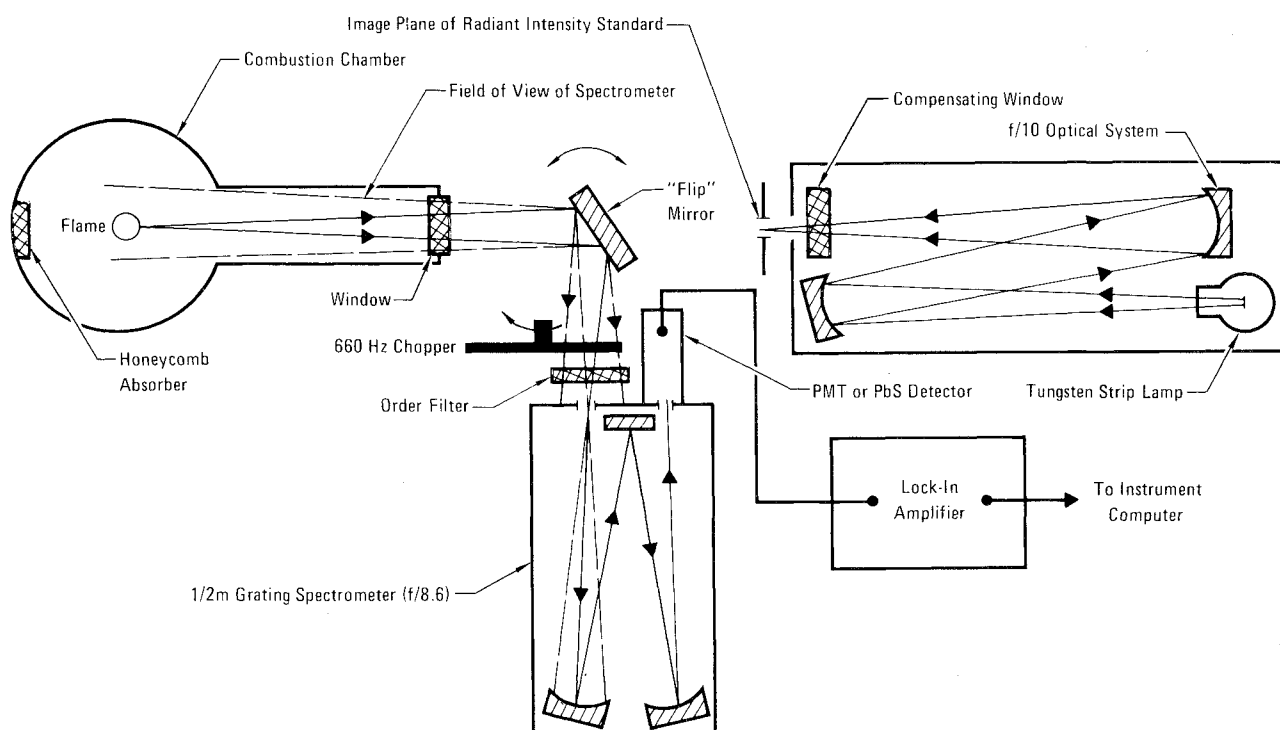


Fig. 2 Optical system for spectral radiant intensity measurements (0.2–2.6  $\mu\text{m}$ )

flame was made, a calibration scan was recorded on the tape, and a CDC 6500 computer was used to convert the data to graphical plots of spectral radiant intensity for each flame. This conversion was made with the expression

$$J_F(\lambda) = J_s(\lambda) \frac{V_F(\lambda)}{V_s(\lambda)} \left( \frac{d_F}{d_s} \right)^2 (\text{W nm}^{-1} \text{sr}^{-1}) \quad (1)$$

where  $J_s(\lambda)$  is the spectral radiant intensity of the calibration source ( $\text{W nm}^{-1} \text{sr}^{-1}$ );  $V_F(\lambda)$ ,  $V_s(\lambda)$  are the voltages generated in the computer memory by the flame and the calibration source, respectively ( $V$ ); and  $d_F$ ,  $d_s$  are the distances of the flame and calibration source from the entrance aperture of the spectrometer (m).

At each wavelength the value of  $J_s(\lambda)$  was computed from Planck's expression for the radiance of a blackbody  $N_s(\lambda)$

$$J_s(\lambda) = A_s \cdot N_s(\lambda) = \frac{A_s}{\pi} \cdot \frac{C_1}{\lambda^5} \left[ \exp\left(\frac{C_2}{\lambda T(\lambda)}\right) - 1 \right]^{-1} \quad (2)$$

where  $A_s$  is the area of the exit aperture on the calibration source ( $\text{m}^2$ );  $T(\lambda)$  is the equivalent blackbody temperature of the calibration source at wavelength  $\lambda$  (K); and  $C_1$ ,  $C_2$  are constants. The values of  $T(\lambda)$  were determined from the NBS-traceable calibration of the radiance standard.

### Experimental Results

The spectral radiant intensity of a 17.5 cm tall diffusion flame of JP-4 was measured in ten separate spectral ranges at four simulated altitudes. In order to ease the presentation of this information, the computer-generated spectral radiant intensity curves were reduced to composite curves using a Hewlett-Packard 9810A Programmable Computer equipped with digitizing and plotting accessories.

The experimental results are discussed in three sections corresponding to the ultraviolet, the visible and near infrared, and the far infrared spectral regions.

Table 1 Summary of the optical components used in the spectral radiant intensity measurements

Spectral Range	Spectrometer	Order Filters*	Grating		Bandwidth	Detector
			Ruling	Blaze		
200-243 nm	Jarrell Ash	None	1180 $\ell/\text{mm}$	300 nm	1.6 nm	Photomultiplier - Varian G-26H215
240-283 nm	1/2 m Grating Spectrometer	None		300 nm		
280-323 nm		None		300 nm		
300-471 nm	Jarrell Ash	Soda Glass	1180 $\ell/\text{mm}$	300 nm	1.6 nm	Photomultiplier - EMI 9558 QC
470-641 nm	1/2 m Grating Spectrometer	440 nm <sup>(1)</sup>		750 nm		
640-811 nm		440 nm <sup>(1)</sup>		750 nm		
0.80-1.49 $\mu\text{m}$	Jarrell Ash	0.76 $\mu\text{m}$ <sup>(2)</sup>	295 $\ell/\text{mm}$	1.5 $\mu\text{m}$	19.2 nm	Lead Sulphide - Kodak Cell
1.48-2.16 $\mu\text{m}$	1/2 m Grating Spectrometer	1.00 $\mu\text{m}$ <sup>(3)</sup>		1.5 $\mu\text{m}$		
2.00-2.65 $\mu\text{m}$		1.80 $\mu\text{m}$ <sup>(4)</sup>		1.5 $\mu\text{m}$		
2.0-15.0 $\mu\text{m}$	Block Engineering Interferometric Spectrometer				40 $\text{cm}^{-1}$	Thermistor

\* Wavelengths listed are cut-on values of long wavelength pass (L.W.P.) filters: (1) Corning Glass CS 3-72, (2) OCLI L.W.P. Interference Filter, (3) Corning Glass CS 4-71, (4) OCLI L.W.P. Interference Filter.

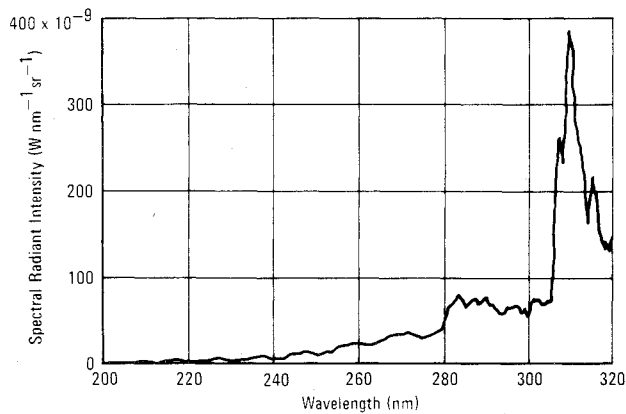


Fig. 3 Spectral radiant intensity of JP-4 burning at sea level (200 nm–320 nm).

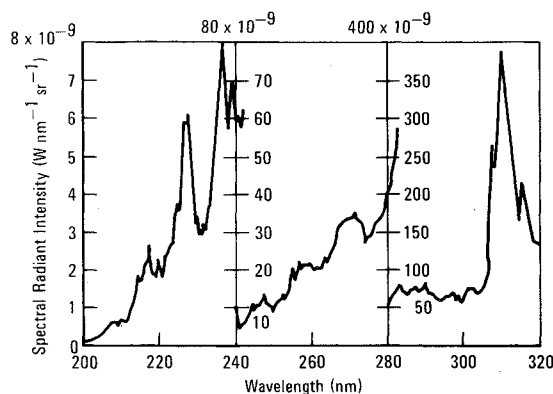


Fig. 4 Spectral radiant intensity of JP-4 burning at sea level—expanded (200–320 nm).

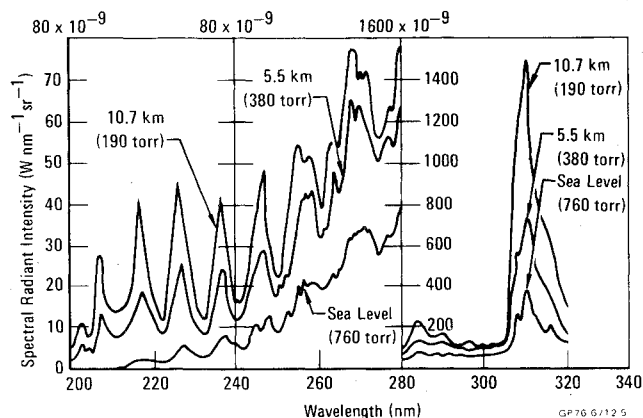


Fig. 5 Ultraviolet emissions from JP-4 burning at various altitudes.

#### Ultraviolet Emission Spectra

This region is of considerable interest to designers, manufacturers, and users of aircraft fire detectors because of the increasing use of solar-blind, ultraviolet sensors as the basic element in detection systems. The wavelengths of particular interest lie between a lower limit of approximately 200 nm, set by the absorption edge of many detector window materials and the absorption by atmospheric oxygen, and an upper limit of 280 nm, above which solar radiation penetrates the ozone belts around the earth. In this study the ultraviolet measurements were extended out to 320 nm to include the strong emission bands characteristic of the OH radical at 310 nm.

Figure 3 shows the spectral radiant intensity of JP-4 burning at sea level, the same data being presented in Fig. 4

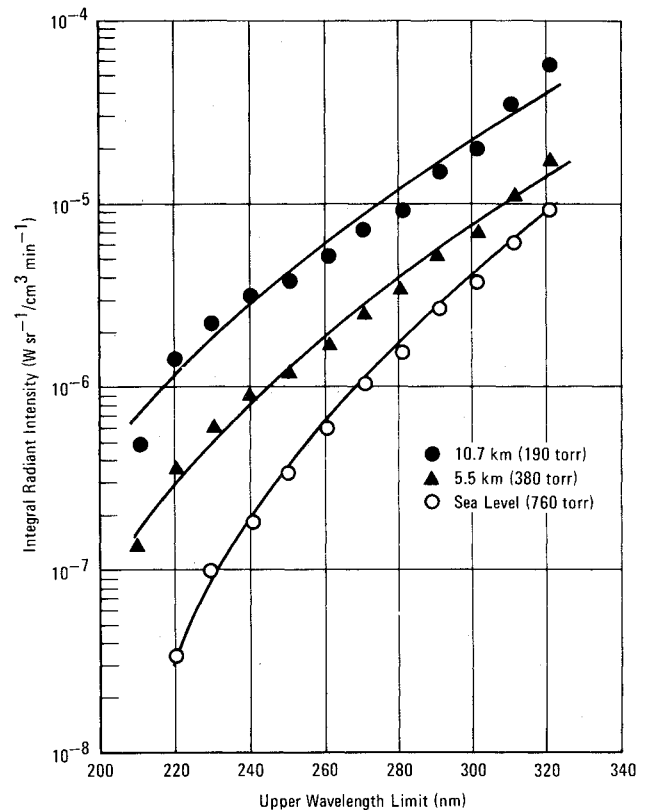


Fig. 6 Integral radiant intensity of JP-4 flames burning at various altitudes (data normalized for unit fuel flowrate).

with expanded ordinates. The emissions in this region are seen to exhibit quite intense band structure, with the spectral radiant intensity varying by more than three orders of magnitude across the spectral range.

Spectral emission data were also recorded at 5.5 km (380 torr) and 10.7 km (190 torr), and the results are shown in Fig. 5.

It is apparent that the radiation emitted in the ultraviolet region by JP-4 flames increases with increasing altitude. This increase is particularly marked at the peaks in the spectra; the peak at 215 nm is more than ten times stronger at 10.7 km than at sea level.

Spectral radiant intensity curves such as those illustrated in Figs. 3–5 provide important information on the distribution of the emitted radiation. However, the designer of a fire detection system must be concerned with the total energy emitted by the fire in the spectral range of the sensor. This range is established by the 200 nm lower limit of the transparency of the window materials and the atmosphere, and the upper wavelength limit of the sensor sensitivity. This latter parameter can be controlled by the selection and preparation of the photosensitive surfaces.

To assist the designer, the spectral data were converted to values for the integral radiant intensity  $P_F(\lambda)$ . This parameter is defined by the expression

$$P_F(\lambda) = \int_{200}^{\lambda} J_F(\lambda) d\lambda \quad (\text{Wsr}^{-1})$$

where  $J_F(\lambda)$  ( $\text{Wnm}^{-1}\text{sr}^{-1}$ ) is the spectral radiant intensity of the flame. The values of  $P_F(\lambda)$  represent the total energy emitted by the flame in the wavelength range between 200 nm and  $\lambda$ , and, therefore, the energy available for detection by a sensor which has a long wavelength cutoff of  $\lambda$ . Values of  $P_F(\lambda)$  for JP-4 burning at various altitudes are illustrated in Fig. 6. The lower, sea-level curve was obtained by a series of integrations of the area under the sea-level curves in Fig. 4,

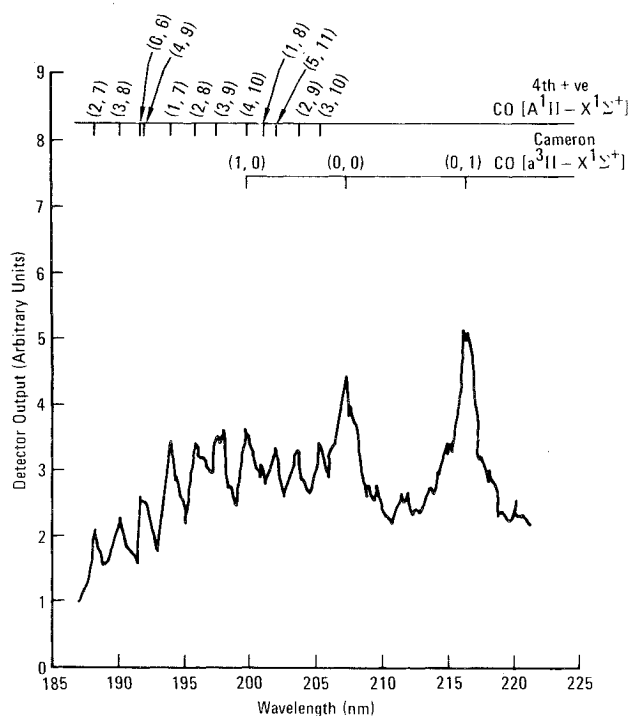


Fig. 7 Emission spectra of JP-4 burning at 10.7 km (185-220 nm).

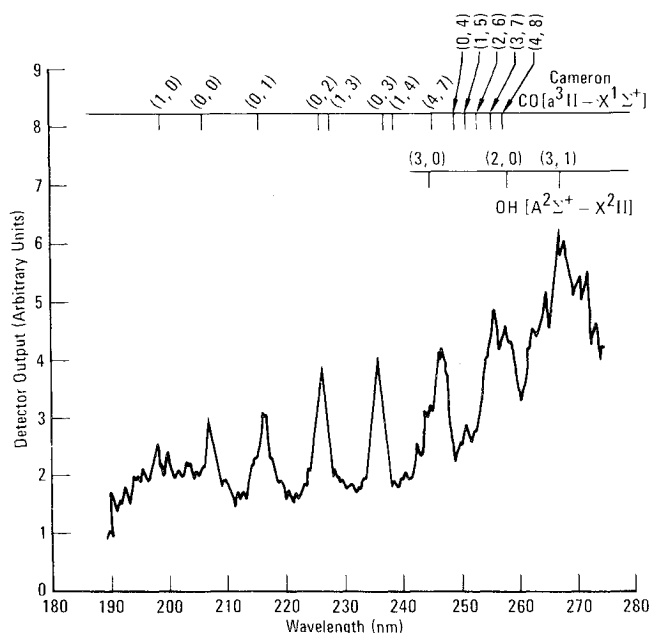


Fig. 8 Emission spectra of JP-4 burning at 10.7 km (190-275 nm).

using the Hewlett-Packard 9810A Programmable Calculator. Each of the high-altitude curves in Fig. 6 was derived from appropriate radiant intensity plots similar to those illustrated in Fig. 5. The curves in Fig. 6 emphasize the increase in the ultraviolet emissions from JP-4 flames at high altitudes; there is an order-of-magnitude difference between the energy emitted at 10.7 km and that emitted at sea level. The energy available for detection is also a critical function of the upper wavelength limit of the sensor used; for example, a detector responding to wavelengths up to 280 nm will receive twice the detectable radiation to which a 260 nm-limited detector would respond.

To aid in the identification of the emitting species responsible for the pronounced band structure in the ultraviolet region, two additional spectral scans were recorded. For these scans the bandwidth of the spectrometer

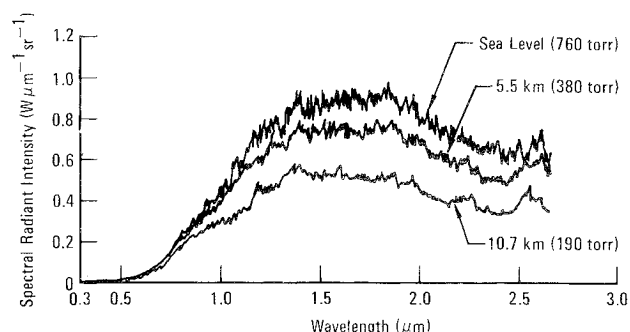


Fig. 9 Visible and near-infrared emissions from JP-4 burning at various altitudes.

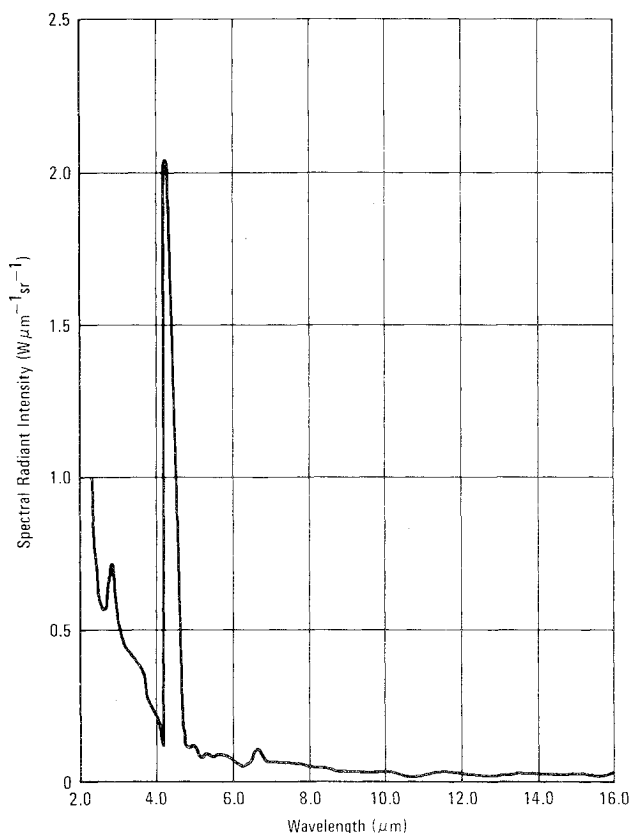


Fig. 10 Far-infrared emissions from JP-4 burning at sea level.

was decreased to 0.64 nm (from 1.6 nm), the scanning speed was slowed to 5 nm/min (from 12.5 nm/min) and electrical time constants of up to 3 sec were used (cf. 300 msec). Reproductions of the raw data curves in Figs. 7 and 8 have been marked with the characteristic wavelengths of several spectral systems. It is apparent that the strong bands emitted in the 200-280 nm region are due to a combination of the Cameron Bands of the CO radical ( $A^3II-X^1\Sigma^+$ ) (Ref. 1) and the ( $A^2\Sigma^+-X^2II$ ) (Ref. 2) system of the OH radical. Below 200 nm (Fig. 7) the finely divided structure is attributed to the 4th positive system of CO ( $A^1II-X^1\Sigma^+$ ) (Ref. 3).

#### Visible and Near-Infrared Emission Spectra (300 nm-2.6 μm)

Despite the high background radiation in this wavelength range in many applications, several successful radiation fire detection systems utilize devices sensitive to visible and near-infrared radiation.

The spectral data, recorded in six separate but consecutive scans at three separate altitudes, were combined using the HP-9810A to produce Fig. 9. These composite curves emphasize the featureless nature of the spectra, apart from a suggestion of an emission band near 2.7 μm. It is apparent that the

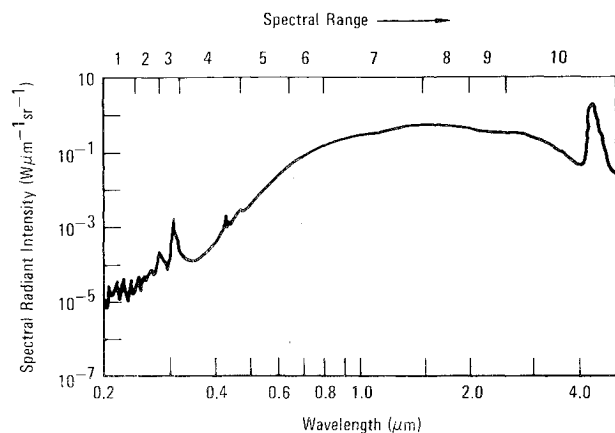


Fig. 11 Optical emissions from JP-4 burning at 10.7 km (190 torr).

radiation emitted by the flames at these wavelengths originated from hot particles of unburned carbon in the diffusion flame. This is the source of the familiar yellow color of a candle flame and other diffusion flames, although these measurements indicate that the bulk of the radiation is emitted in the near infrared, rather than at visible wavelengths. The maxima in the emission curves occurred between  $1.5\ \mu\text{m}$  and  $2.0\ \mu\text{m}$ , indicating that the characteristic temperature of the carbon particles was in the 1500–2000 K range.

It is seen that in the visible and near infrared region the spectral radiant intensity from burning JP-4 decreases at higher altitudes.

#### Far-Infrared Emission Spectra (2.5–15 $\mu\text{m}$ )

Fire detectors sensitive to wavelengths longer than  $2\ \mu\text{m}$  are not yet in common use in aircraft but the lack of significant solar radiation in this range makes such devices potentially useful. Hot surfaces in an aircraft engine compartment can emit strongly at these wavelengths but such background might be discriminated against.

Shown in Fig. 10 is the spectral radiant intensity from JP-4 burning at sea level. The dominant emission band centered at

$4.4\ \mu\text{m}$  is characteristic of the excited  $\text{CO}_2$  molecule. A smaller peak at  $2.7\ \mu\text{m}$  is characteristic of the excited  $\text{CO}_2$  and  $\text{H}_2\text{O}$  molecules. The continuum between  $2.7$  and  $4.0\ \mu\text{m}$  is the long wavelength end of the previously discussed blackbody-type emission of the hot carbon particles in the flame.<sup>3</sup> The far-infrared emission data recorded at other altitudes are remarkably similar to those shown in Fig. 10.

#### Summary

In the course of the program the emissions from JP-4 flames were recorded over almost the complete electromagnetic spectrum that can be effectively utilized for fire detection. A composite curve for the data taken at 10.7 km is included as Fig. 11 and, despite the ten separate ranges over which the spectrum was scanned, the continuity of the curve is good.

It is apparent that the bulk of the energy emitted by a JP-4 diffusion flame is blackbody radiation from the hot carbon particles in the flame. The visible/infrared radiation has been observed to decrease in intensity with decreasing pressure, i.e., increasing altitude, while the intensity of the prominent ultraviolet and infrared emission bands was observed to increase at high altitude. Although the work discussed in this paper was restricted to JP-4 fuel, other studies have shown that the emission spectra from most of the commonly used fuels and hydraulic fluids have similar characteristics.

The discrete nature of the spectral emission bands associated with the  $\text{CO}_2$  molecule at  $4.4\ \mu\text{m}$ , and the CO and OH radicals at ultraviolet wavelengths, should lend these bands to a discriminating optical fire detector. Current developments center around ultraviolet sensors blind to solar radiation and other sources, but a development effort on a  $4.4\ \mu\text{m}$  system could result in a sensitive, rugged, and inexpensive detector for aircraft applications.

#### References

- <sup>1</sup>Berg, R.E. and Bonne, U., "Combustion Sensors—Phase III," Honeywell, Inc., Boston, Mass., HR-R-64-251-L, Jan. 1967.
- <sup>2</sup>Mavrodineanu, R., *Flame Spectroscopy*, Wiley, New York, 1965, pp. 576–7.
- <sup>3</sup>Gaydon, A.G., *The Spectroscopy of Flames*, Chapman and Hall, London, 1957, pp. 164–178, 238.